Australian Government
Department of Defence
Defence Science and
Technology Organisation

# Reference Assisted TDOA Computation for On-Off Keyed Signals

***Gareth Parker and John Homer***

**Command, Control, Communications and Intelligence Division**

**Defence Science and Technology Organisation**

**DSTO–TR–2457**

## ABSTRACT

This document considers the use of a partially known prototype signal to enhance the time difference of arrival (TDOA) computation for an On-Off Keyed (OOK) signal. It is shown through analysis and simulation that this approach can achieve a considerable reduction in the SNR threshold at which an acceptable rms TDOA spread can be achieved. For a signal transmitted with a carrier frequency that is stable within each observation interval, the threshold improvement can be in excess of 10 dB for a signal of practical interest. A similar degree of improvement was also observed for a signal with a carrier that exhibited frequency drift of up to 0.5 Hz within a 1.5 second interval. Analysis and simulation results are shown to be consistent with computations performed on data acquired from real transmitters.

*Published by*

*DSTO Defence Science and Technology Organisation*
*PO Box 1500*
*Edinburgh, South Australia 5111, Australia*

*Telephone: (08) 7389 5555*
*Facsimile: (08) 7389 6567*


*AR No. AR–014–831*
*August 2010*

***APPROVED FOR PUBLIC RELEASE***

# Reference Assisted TDOA Computation for On-Off Keyed Signals

## Executive Summary

The estimation of the relative delay between a signal component common to that received at two spatially separated antennas is a problem of general interest. This Time Difference of Arrival (TDOA) is usually estimated as the argument of the peak in the cross-correlation computed between the two signals. The variance of this time estimate is dependent on the Signal to Noise Ratio (SNR), including a product term that exacerbates the estimation error when the SNR for both signals is low.

This report considers the use of a prototype signal to enhance the TDOA estimation of a known signal of interest. In this approach, the TDOA is estimated as the difference between two intermediate computations; the TDOA estimates computed between the prototype and each of the two received signals. Each of these intermediate estimates exploits the assumption that the SNR associated with a perfect prototype signal is infinite, which consequently eliminates the SNR product term discussed in the preceding paragraph.

Expressions for the variance of this estimator are derived for the generic case and are further refined for the special cases of Binary Phase Shift Keyed (BPSK) and On-Off Keyed (OOK) modulation types. It is shown through analysis and simulation that this prototype assisted approach can achieve a considerable reduction in the SNR threshold at which an acceptable rms TDOA spread can be achieved. For an OOK signal with a perfect prototype, analysis and simulations show that the threshold improvement can be in excess of 10 dB for a signal of practical interest. These results are shown to be consistent with computations performed on data acquired from real transmitters.

Although the analytical expressions derived in the report relate to the ideal case where the prototype signal is a perfect replica of the transmitted signal, the report acknowledges that the performance enhancement may be compromised when this is not true. Additional simulations are presented that assess the impact of uncertainty in the signal carrier frequency, specifically that it drifts linearly with time over the observation interval. For the simulation parameters, only a slight degradation was observed for a carrier that drifted linearly up to 0.5 Hz over a 1.5 second interval. Further mitigation against the effect of carrier frequency drift, via a high pass filtering technique is also proposed.

An additional contribution of this report is the clarification of the conditions under which a commonly cited expression for TDOA variance holds. That expression, from a seminal paper in the field, was originally introduced with neither proof nor qualification.

# Authors

**Gareth Parker**
*C3ID*

Gareth Parker joined DSTO in December 1987. In 1990 he received a Bachelor of Engineering, with first class honours, in Electrical and Electronic Engineering from Adelaide University. In 2001 he received a PhD from the University of South Australia for research into discrete time frequency domain signal processing. Currently leading the Signals Analysis Discipline in C3ID, his research interests include signal analysis and processing for robust communications.

**John Homer**
*C3ID*

John Homer received the BSc degree in physics from the University of Newcastle, Australia in 1985 and the PhD degree in systems engineering from the Australian National University, Australia in 1995. Between his BSc and Ph.D studies he held a position of Research Engineer at Comalco Research Centre in Melbourne, Australia. Following his PhD studies he has held research positions with The University of Queensland, Veritas DGC Pty Ltd and Katholieke Universiteit Leuven, Belgium and a Senior Lecturing position at the University of Queensland within the School of Information Technology and Electrical Engineering. He has been with DSTO since July 2006, as a Senior Research Engineer. His research interests include signal and image processing, particularly in the application areas of telecommunications, audio and radar.

# Contents



# Appendices

# Glossary

**BPSK** Binary Phase Shift Keyed (modulation)

**CW** Continuous Wave

**DTO** Differential Time Offset

**FFT** Fast Fourier Transform

**IF** Intermediate Frequency

**OOK** On-Off Keyed (modulation)

**RF** Radio Frequency

**SNR** Signal to Noise Ratio

**SOI** Signal Of Interest

**TDOA** Time Difference Of Arrival

# 1 Introduction

The estimation of the relative delay between a signal component common to that received at two spatially separated antennas is a problem of general interest. Specifically, consider the reception of a transmitted signal $s(t)$ by two spatially separated antennas, denoted $x_1(t)$ and $x_2(t)$

$$\begin{aligned} x_1(t) &= s(t) + n_1(t) \\ x_2(t) &= \alpha s(t+D) + n_2(t), \end{aligned} \tag{1}$$

where $n_1(t)$ and $n_2(t)$ are additive noise with arbitrary distribution, $\alpha$ is a scalar coefficient and $D$ is the relative time delay, sometimes known as the Time Difference of Arrival (TDOA) or Differential Time Offset (DTO) [3]. This is often estimated as the argument of the correlation peak $\hat{D} = \arg\max R_{x_1x_2}(\tau)$. If one had the ability to exactly compute this cross correlation function then the approach would be optimal, but when the correlation must be estimated, the optimal (maximum likelihood) approach is to emphasise the energy associated with the signal component by appropriately pre-filtering the $x_1(t)$ and $x_2(t)$ in a *generalised correlation* [2, 5]. In the absence of *a priori* knowledge of the signal and noise characteristics, a pragmatic approach can be as simple as prefiltering the signals to approximately the bandwidth that contains most of the signal energy.

To minimise the sampling rate and consequently the computational complexity, correlation of radio frequency (RF), or high intermediate frequency (IF) signals is often avoided [5] and the correlation is performed on the complex envelopes[1] $\tilde{x}_1(t)$ and $\tilde{x}_2(t)$ so that $\hat{D} = \arg\max \hat{R}_{\tilde{x}_1\tilde{x}_2}(\tau)$. Consider the case where the signal and noise are restricted to within an IF bandwidth $\omega_0 \pm W/2$, where $\omega_0$ and $W$ are the carrier frequency and bandwidth respectively. Then if $\alpha = 1$ and for sufficiently high signal to noise ratio (SNR)[2] the Cramer Rao bound for the variance of the estimation of time delay using complex envelopes is given by [5]

$$\sigma^2_{min} = \left[ \frac{T}{2\pi} \int_{\omega_0 - W/2}^{\omega_0 + W/2} 2SNR(\omega)(\omega - \omega_0)^2 d\omega \right]^{-1}, \tag{2}$$

where

$$SNR(\omega) = \frac{G_{ss}(\omega)/G_{n1n1}(\omega).G_{ss}(\omega)/G_{n2n2}(\omega)}{1 + G_{ss}(\omega)/G_{n1n1}(\omega) + G_{ss}(\omega)/G_{n2n2}(\omega)} \tag{3}$$

and $G_{ss}(\omega)$, $G_{n1n1}(\omega)$ and $G_{n2n2}(\omega)$ are the signal and noise auto-spectra. This can be alternatively phrased in terms of frequency units of Hertz through a change of variables, $\omega = 2\pi f$ and using bandwidth $B_s$ Hz instead of $W$ rad/sec. Then the minimum variance is shown in Appendix A to be

[1] The complex envelope $\tilde{x}_1(t)$ is defined by $x(t) = \text{Real}\{\tilde{\text{x}}_1(\text{t}) \exp(\text{j}2\pi\text{f}_\text{c}\text{t})\}$, where $f_c$ is the carrier frequency of $x(t)$.

[2] There exists a threshold region [4], below which, time delay estimation contains gross ambiguities, but above which, the variance is bounded by the Cramer Rao low bound.

$$\sigma^2_{min} = \left[ 4\pi^2 T \int_{-B_s/2}^{B_s/2} 2f^2 \frac{\tilde{G}_{ss}(f)/\tilde{G}_{n1n1}(f).\tilde{G}_{ss}(f)/\tilde{G}_{n2n2}(f)}{1 + \tilde{G}_{ss}(f)/\tilde{G}_{n1n1}(f) + \tilde{G}_{ss}(f)/\tilde{G}_{n2n2}(f)} df \right]^{-1}, \quad (4)$$

where $\tilde{G}_{ss}(f) = G_{ss}(f + f_c)$ etc.

Equation (4) simplifies further, in a way that provides greater insight into the problem, as well as allowing a better comparison with commonly accepted literature [3] by considering the case where the noise spectra ($\tilde{G}_{n1n1}(f) = N_1$ and $\tilde{G}_{n2n2}(f) = N_2$) are white within the bandwidth $B_s$ Hz. If the signal has total signal power $p$, then the signal to noise ratio associated with $x_1(t)$ and $x_2(t)$ is respectively $\gamma_1 = p/BN_1$ and $\gamma_2 = p/BN_2$, where $B \approx B_s$ is the equivalent noise bandwidth. Then we can write $\tilde{G}_{n1n1}(f) = p/B\gamma_1$ and $\tilde{G}_{n2n2}(f) = p/B\gamma_2$ so that, as shown in Appendix A,

$$\sigma^2_{min} = \frac{p}{4\pi^2 TB} \left[ \int_{-B_s/2}^{B_s/2} f^2 \tilde{G}_{ss}(f) \gamma_{eq}(f) df \right]^{-1}, \quad (5)$$

where

$$\gamma_{eq}(f) = \frac{2\gamma_1\gamma_2}{p/B\tilde{G}_{ss}(f) + \gamma_1 + \gamma_2}, \quad (6)$$

which can be interpreted as an equivalent SNR associated with the generalised cross-correlation between $x_1(t)$ and $x_2(t)$. This equivalent SNR is always poorer than the individual SNRs, but is significantly less when both $\gamma_1$ and $\gamma_2$ are both less than one. As an example, consider the case where the *signal* has a flat power spectrum between $-B/2$ and $B/2$. Then $p = B\tilde{G}_{ss}(f)$ and the equivalent SNR can be expressed in a form consistent with [3] [3] as

$$\frac{1}{\gamma_{eq}} = \frac{1}{2}\left( \frac{1}{\gamma_1} + \frac{1}{\gamma_2} + \frac{1}{\gamma_1\gamma_2} \right). \quad (7)$$

If $\gamma_1 = \gamma_2 = 10$ (10 dB) then the equivalent SNR $\gamma_{eq} = 4.8$ (6.8 dB) and the cross-term $\gamma_1\gamma_2$ has contributed almost nothing (evaluation of (7) without the cross-term would yield a 7 dB equivalent SNR). On the other hand, if the SNR on the two received signals is $\gamma_1 = \gamma_2 = 0.1$ (-10 dB) then the equivalent SNR is $\gamma_{eq} = 0.0083$ or -20.8 dB and the cross-term has had a considerable effect (evaluation of (7) without the cross-term would yield a -13 dB equivalent SNR).

Fortunately, it will be shown in the next section that the impact of the cross-term in (7) can be lessened by exploiting properties of the transmitted signal in a 'synthetic' reference.

[3] This expression for equivalent SNR, along with other related expressions (eq. equation B2), is given in the broadly cited paper by Stein [3] without proof, nor qualification of the conditions under which it applies. Some of these conditions are given consideration in Appendix B.

# 2 Synthetic TDOA estimation

Assume that the receivers can generate an imperfect but noiseless copy, $r(t)$ of the transmitted signal, where

$$r(t) = a(t)s(t) + e(t) \tag{8}$$

and where $a(t)$ and $e(t)$ represent the multiplicative and additive errors in the estimation of $s(t)$. The TDOA can then be estimated as

$$\hat{D} = D_{1r} - D_{2r} \tag{9}$$

where $D_{1r}$ and $D_{2r}$ are the arguments of the peaks in each of $R_{x_1r}(\tau)$ and $R_{x_2r}(\tau)$, exploiting the observation that the timing uncertainty in $r(t)$ is common to both correlation functions.

The estimate of the TDOA between $x_1(t)$ and $r(t)$ for the case of a perfect reference signal, where $a(t)$ is a constant and $e(t) = 0$ has an equivalent SNR equal to $\gamma_{1r} = 2\gamma_1$, by substituting $\gamma_2 = \infty$ into (6). An analogous error applies to the estimation of the TDOA between the second signal and the reference. Under the assumption that the errors on each of these TDOA estimates can be modelled as zero mean, identically distributed random variables, it follows that the variance of the difference in (9) is equal to the sum of the individual variances. Consequently, for a perfect reference signal and when the noise is white, the variance of the TDOA error is

$$\begin{aligned}
\sigma^2_{synth} &\geq \sigma^2_{1r} + \sigma^2_{2r} \\
&= \frac{p}{4\pi^2 TB}\left(\left[\int_{-B_s/2}^{B_s/2} f^2 \tilde{G}_{ss}(f) 2\gamma_1 df\right]^{-1} + \left[\int_{-B_s/2}^{B_s/2} f^2 \tilde{G}_{ss}(f) 2\gamma_2 df\right]^{-1}\right) \\
&= \frac{p}{4\pi^2 TB}\left[\int_{-B_s/2}^{B_s/2} f^2 \tilde{G}_{ss}(f) df\right]^{-1}\left(\frac{1}{2\gamma_1} + \frac{1}{2\gamma_2}\right),
\end{aligned} \tag{10}$$

which has the same form as equation (5), for the direct TDOA estimation but with

$$\frac{1}{\gamma_{synth}} = \frac{1}{2}\left(\frac{1}{\gamma_1} + \frac{1}{\gamma_2}\right). \tag{11}$$

This is identical to equation (7) for direct TDOA estimation, but without the cross-term that was identified as being most significant if $\gamma_1$ and/or $\gamma_2$ is small. It is noteworthy that for synthetic TDOA estimation, and assuming a perfect reference, the equivalent SNR is independent of frequency, irrespective of the power spectral shape of the signal of interest. The dependence of the minimum variance on the spectral shape of the signal of interest can be extracted from the variance expression by observing that $p = \int_{-B_s/2}^{B_s/2} G_{ss}(f) df$ and employing the definition of 'rms radian frequency' [3],

$$\beta = 2\pi\left[\frac{\int_{-\infty}^{\infty} f^2 \tilde{G}_{ss}(f) df}{\int_{-\infty}^{\infty} \tilde{G}_{ss}(f) df}\right]^{1/2}. \tag{12}$$

Then the minimum variance for the synthetic estimation of TDOA is the simplification of (5),

$$\sigma^2_{min} = \frac{1}{\beta^2 TB\gamma_{synth}}. \tag{13}$$

Although in general, the equivalent SNR for 'direct' TDOA estimation is not independent of frequency, under certain conditions frequency independence is achieved, or approximately achieved, and a similar simplification is possible. Appendix B shows that such cases include when the signal of interest is white or when the SNR is high, with a lower variance bound (B2) having similar form to (13).

# 3 Simulation results

In this section, the results of simulations are presented, that better illuminate the potential benefit of using the synthetic technique for the estimation of TDOA. Although the fundamental focus of this report is on TDOA estimation for an OOK signal, results are first presented for two other, simpler cases. First, a white signal of interest is considered, as this allows for a very close approximation to the maximum likelihood estimator to be used without requiring a complicated prefiltering. The second special case is for a Binary Phase Shift Keyed (BPSK) signal, since it also has a nicely defined power spectrum and can be considered as a constituent component of an OOK signal[4].

## 3.1 White Gaussian signal of interest

Simulation results are presented here for the special case where the signal of interest is a *real*, white, Gaussian noise-like signal. The signal is centered exactly at baseband and is processed in the presence of complex Gaussian white noise[5]. A 312.5 kHz sampling rate and integration period $T = 1.5$ sec were used. The signal and noise were bandlimited to within approximately $\pm$ 5 kHz bandwidth using a 512-tap FIR filter[6]. The noise bandwidth $B$ and the rms radian frequency $\beta$ were computed to equal 9.6 kHz and 1.74e3 rad/sec respectively. (The filter frequency response is shown later in Figure 3.)

Figure 1 shows the simulation results for the direct and synthetic TDOA estimation represented by circles and crosses respectively. Each data point was computed using 100 simulation runs and for the direct TDOA computation below -15 dB SNR, any outlier TDOA values in excess of 100 $\mu$sec were excluded from the rms computation; such outliers are the result of gross errors in the TDOA estimate, and represent behaviour below the threshold at which the TDOA estimate is ambiguous and not a noisy displacement from true correlation peak [4].

The lower bound for the synthetic estimation, predicted from the application of equa-

[4] An OOK signal can be represented as the sum of CW and BPSK components.

[5] The use of a noise source that is complex may at first seem questionable, but is representative of a real world scenario, in which the IF noise would in general be asymmetric about the carrier frequency.

[6] generated with the Matlab routine 'fir1'

tions (13) and (11) is shown by the solid curve and the lower bound on the direct estimation, given by Stein's expression, (7) and (B2), is shown as the dashed curve.

There is a very close agreement between the simulation results and the theoretical bounds for this simple case where both the signal and noise have the same shaped, flat power spectra. If the received signal (and noise) is bandlimited by a square IF filter, theory suggests that optimal 'direct' TDOA estimation is achieved with a conventional correlation. The performance advantage that synthetic estimation offers in this case is clear and grows as SNR is reduced. As an example, it can be seen that synthetic estimation improves the rms TDOA error by extending the threshold at which an 8 $\mu$sec error is achieved by around 10 dB.

Figure 2 is included here to show how the various other expressions for the lower bound on the rms error for direct TDOA estimation give subtly differing curves. The black curve corresponds to the application of Stein's equation (7), using $\beta$ computed from numerical integration, as in Figure 1. The dotted curve corresponds to the use of equation (6), with the equivalent SNR $\gamma$ also computed from the exact filter frequency response. That this curve doesn't match the simulation data as well as the application of (7) is because although the signal and noise have the same spectral shape, the noise is implicitly modelled as having been filtered by a brick wall filter, yet the signal is being modelled 'exactly'; the alternative use of the brick wall response in (6) yields the same result as the application of (7). The overlaid green and dashed blue traces respectively correspond to the application of (6) and (7) with the assumption of a brick wall filter response. The red curve corresponds to the low SNR approximation of Appendix B.3.

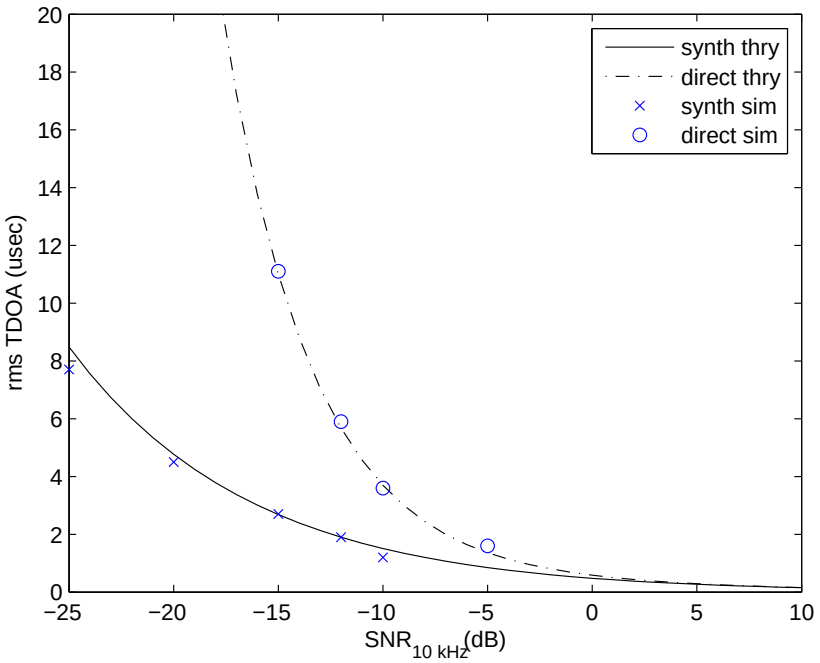


***Figure 1:*** *rms TDOA accuracy associated with a white noise signal.*

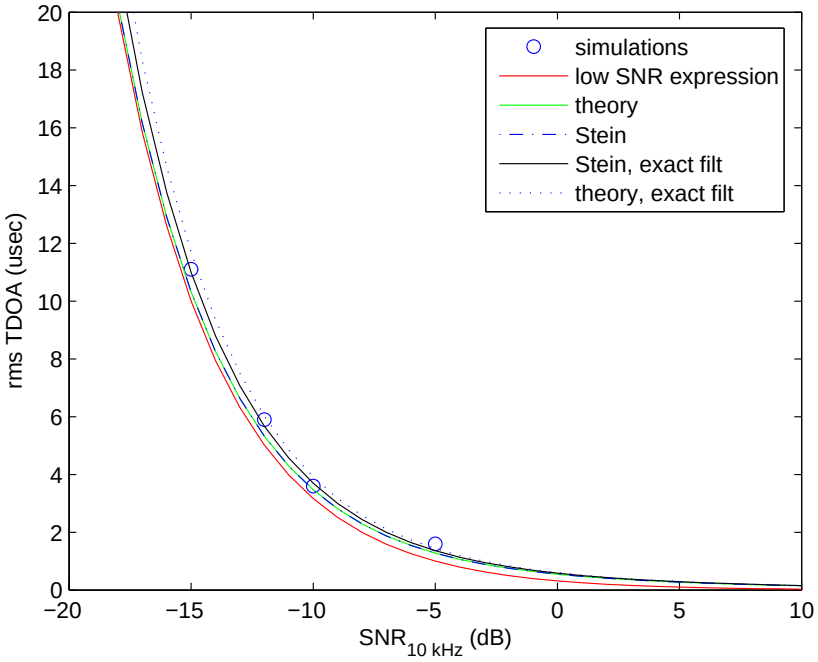


***Figure 2:*** *rms TDOA accuracy for a white signal, direct estimation.*

## 3.2 BPSK signal

This section considers results for a BPSK signal of interest, using a similar approach to that in 3.1, but with a 5400 baud, baseband BPSK signal. The rms radian frequency $\beta$ was numerically computed to equal 11.3 krad/sec, including the effect of the receiver filter frequency response[7], shown in Figure 3 along with the filtered BPSK power spectrum. Each data point was again based on 100 simulation runs.

Figure 4 shows the simulation results for the direct and synthetic computation as circles and crosses, respectively. The theoretical lower rms bound for synthetic computation is shown as the solid black curve and closely matches the simulation results.

The theoretical lower bound for the direct computation, suggested by the application of Stein's equations (7) and (B2), is shown by the dotted curve and the bound suggested by the application of (5) and (6) is shown as the dashed curve. Each of the theoretical curves were evaluated using a numerical evaluation of the true IF filter impulse response in the computation of the parameters $\gamma$, $\beta$ and $B$.

The consistency between the theoretical curves for the direct TDOA estimation is close. The application of equations (5) and (6) has the best agreement with the simulation results, which is satisfying since the BPSK signal has a spectrum that significantly deviates from the flat shape necessary for the general application of Stein's expression (7) for equivalent

[7]For the BPSK signal, $\beta$ is the same to the first decimal place, if the true filter frequency response is used or if it is approximated by a 'brick wall' response, since the BPSK spectral shape dominates the filtered spectrum.

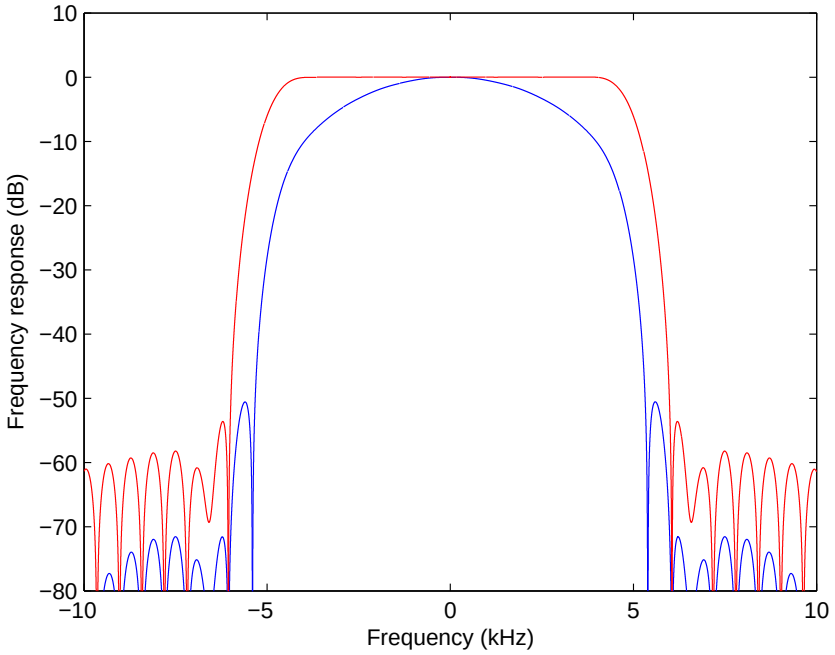


***Figure 3:*** *Power spectrum of filtered BPSK signal (blue) and filter frequency response (red).*

SNR to hold. However, the same degree of consistency between simulation and analysis has not been achieved for the direct computation as was the case for a white noise signal, due to the non-ideal prefiltering of the 'received' signal in the simulations. Recall that as indicated in section 1, the maximum likelihood 'direct' estimator is only achieved through prefiltering the received signals with a filter having an impulse response proportional to the (square root of the) input SNR spectral shape [5], which is not the case here.

## 3.3 OOK signal

The theoretical variance bound for TDOA estimation through correlation of complex envelopes of an OOK signal is derived in Appendix C. The analysis recognises that an OOK signal can be considered as the sum of equal energy BPSK and continuous wave (CW) signal components, but that the CW component makes no contribution to the TDOA estimation[8]. The CW component is explicitly discounted from the analysis by basing the variance bound on the BPSK component only. It is shown in Appendix C that within the receiver bandwidth $B_s$, the SNR associated with the BPSK component is related to the SNR of the OOK signal by

$$\gamma_{BPSK_{B_s}} = \frac{\psi}{1+\psi}\gamma_{OOK_{B_s}}, \tag{14}$$

[8]The correlation function between two tones of identical frequency has no distinct peak.

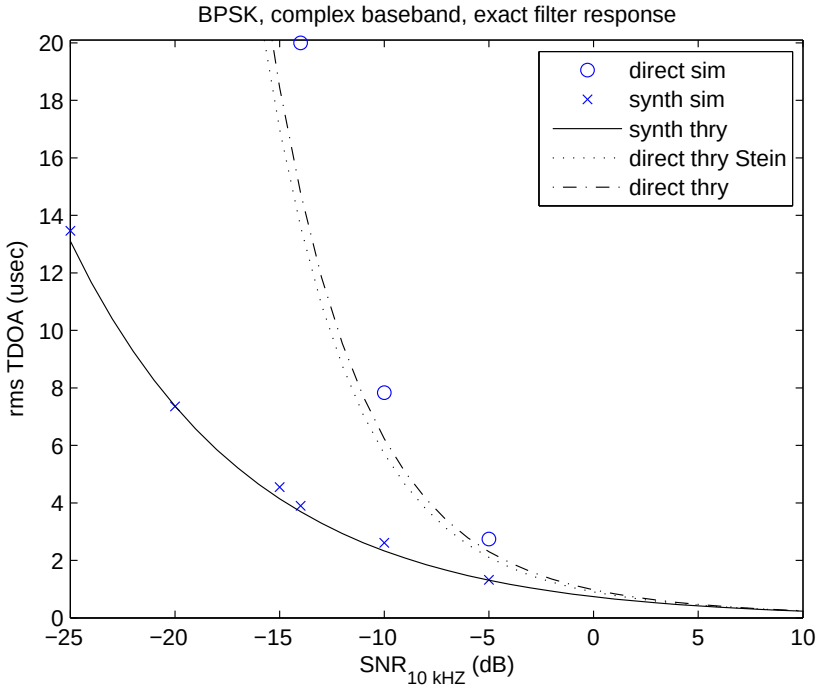


***Figure 4:*** *rms TDOA accuracy for a BPSK signal.*

where

$$\psi = \frac{\sigma^2_{BPSK_{B_s}}}{\sigma^2_{BPSK_\infty}} \tag{15}$$

and where $\sigma^2_{BPSK_{B_s}}$ and $\sigma^2_{BPSK_\infty}$ are the respective variances of the BPSK signal component within the bandwidth $B_s$ and over the theoretical, infinite bandwidth. Using the rms radian frequency for a BPSK signal, $\beta_{BPSK}$ and substituting (14) into equation (13) gives the variance bound for the synthetic approach. The bound for the direct correlation is similarly found using (5) or the applicable special case equation from Appendix B. A second analytical approach is included in Appendix C.2 which makes explicit use of the SNR of the OOK signal and develops a corresponding expression for its rms radian frequency. As discussed in Appendix C.2, the performance of this second approach is inferior.

The performance bounds have been evaluated for OOK signalling at $f_b = 5400$ Hz, sampling frequency $f_s = 312.5$ kHz, a 0 Hz carrier (i.e. basebanded signal), an observation period $T = 1.5$ sec, $B_s \approx 10$ kHz ($\pm 5$ kHz) and additive white Gaussian noise. Figure 5 shows the rms error expected for the synthetic TDOA computation (using (11) and (13)) and the rms error for direct computation using (5) and (6). The parameters $\beta$, $B$ and $\gamma$ were numerically computed using the exact equivalent baseband frequency response of the bandlimiting filter, generated by the Matlab 'fir1' function, with 512 taps. Like the results for white or BPSK signals, the curves portray a significant advantage in the threshold at which a given TDOA accuracy can be achieved through using the synthetic computation. This advantage can be in excess of 10 dB at low SNR.

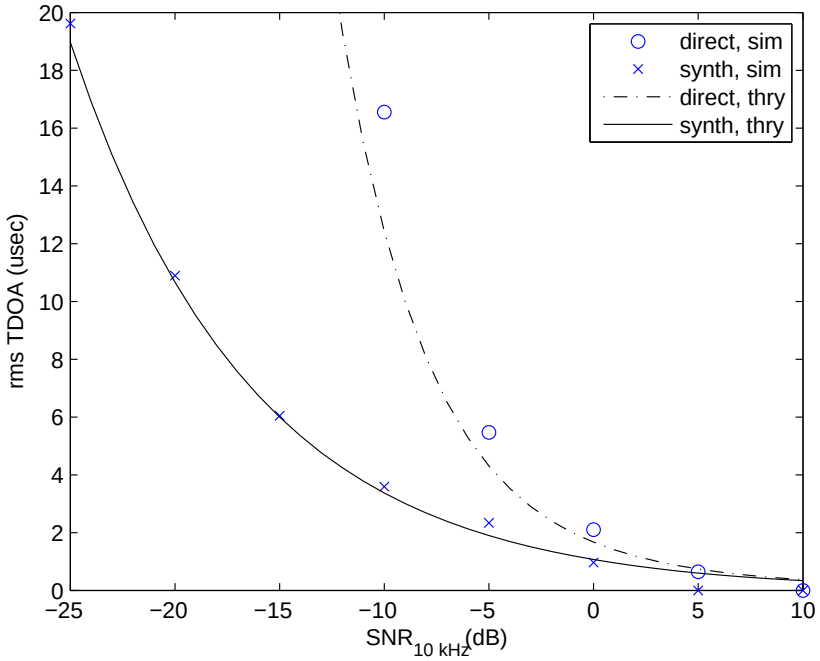


***Figure 5:*** *Theoretical and experimental rms TDOA accuracy associated with an OOK signal, with 0Hz carrier frequency.*

# 4 Implications of an imperfect reference signal

In practise the reference signal will exhibit some error and one of the principle sources of uncertainty will likely be an imperfectly estimated carrier. This section examines the effects of carrier estimation error on the performance of synthetic TDOA computation.

## 4.1 Considerations for a non-zero carrier frequency

If the signal of interest (SOI) is translated to baseband with some residual frequency offset, the use of the expression for rms radian frequency (12) will incur an error. To examine the effect of this, simulations were conducted on a signal set incorporating the OOK SOI from section 3, but with a carrier frequency that was randomly selected within the arbitrary range 10 to 333 Hz[9]. The performance, shown in Figure 6 can be seen to be nearly identical to that shown in Figure 5, for a 0 Hz carrier. This suggests that the slight asymmetry of the associated power spectrum has little impact on the modelled TDOA accuracy.

[9]The simulations were performed using a routine that was written to facilitate the observation of effects associated with having a linearly drifting carrier frequency. The drift was achieved using a Matlab 'chirp' function, which was suspected of not performing well with a notionally zero frequency start, hence the lower 10 Hz limit. In each of 100 iterations, a different carrier frequency was randomly chosen.

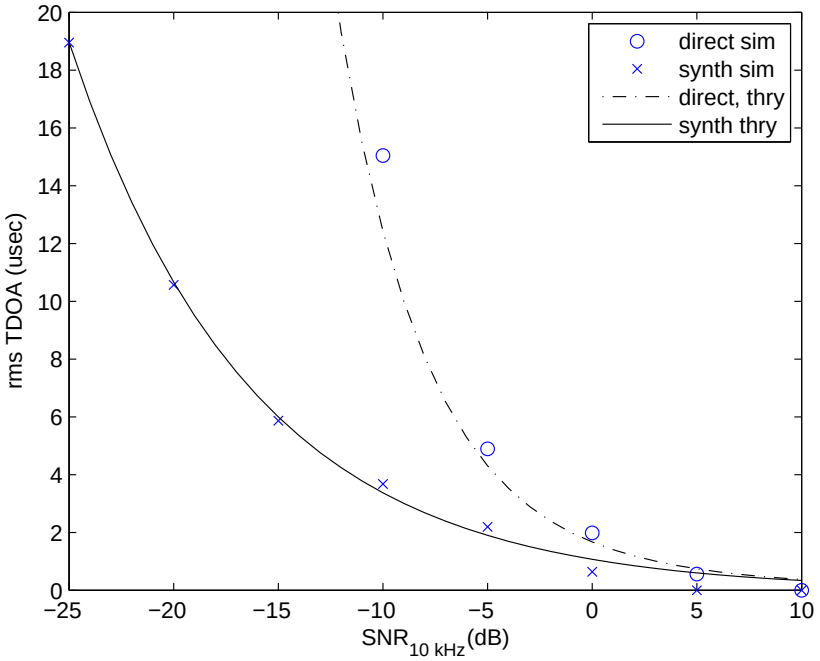


***Figure 6:*** *Theoretical and experimental rms TDOA accuracy associated with an OOK signal, random carrier frequency.*

## 4.2 Simulations with imperfect carrier frequency estimation

A more significant practicality is that the SOI may have a carrier frequency uncertainty that drifts with time. A simple and effective estimator for the carrier frequency of an OOK signal is proportional to the argument of the peak in the estimated power spectrum, usually computed using fast Fourier transforms (FFTs). For a stable carrier frequency, an FFT-based estimator will provide increased accuracy as the block length is increased. However for a drifting carrier, the accuracy suffers if the block length extends too far. Although the degradation to the accuracy of the TDOA estimate for a drifting carrier is a function of the way in which the carrier frequency drifts, a useful figure of merit is the performance in response to a carrier that drifts linearly over the integration interval.

Once again, consider the OOK signal from previous simulations. However, now consider that the carrier frequency is known at the start of the integration interval but that it drifts linearly from there after. Figure 7 shows how the accuracy of the TDOA estimate suffers as the maximum frequency drift increases from 0Hz up to 1.0 Hz. The curve for 1.0 Hz can be seen to have a poorer result than for the TDOA estimated directly from the correlation between the two noisy received signals; this is an example of a behaviour that is conjectured to generally occur when the drift exceeds approximately the reciprocal of the integration period. Such carrier frequency drift affects the quality of the correlation in various ways, including a reduction in the maximum correlation peak. Another source of performance degradation is illustrated in Figure 8, which shows examples of the impact on the estimated correlation function for increasing drift rates.

The magnitude of the correlation function for 0.25 Hz drift has a similar shape to that expected for a steady carrier. However, as the drift increases, the shape of the correlation function begins to grow more rounded and with an increasing number of 'lobes'. Because the magnitude of these lobes can be large compared with the level of the 'true' peak[10] an ambiguity of considerable degree can arise. This is particularly clear in Figure 8 for 1.0 Hz drift, where an ambiguity of around 0.5 sec could exist, through the confusion of the 'true' peak at 1.5 sec with a spurious peak at around 1.0 sec.

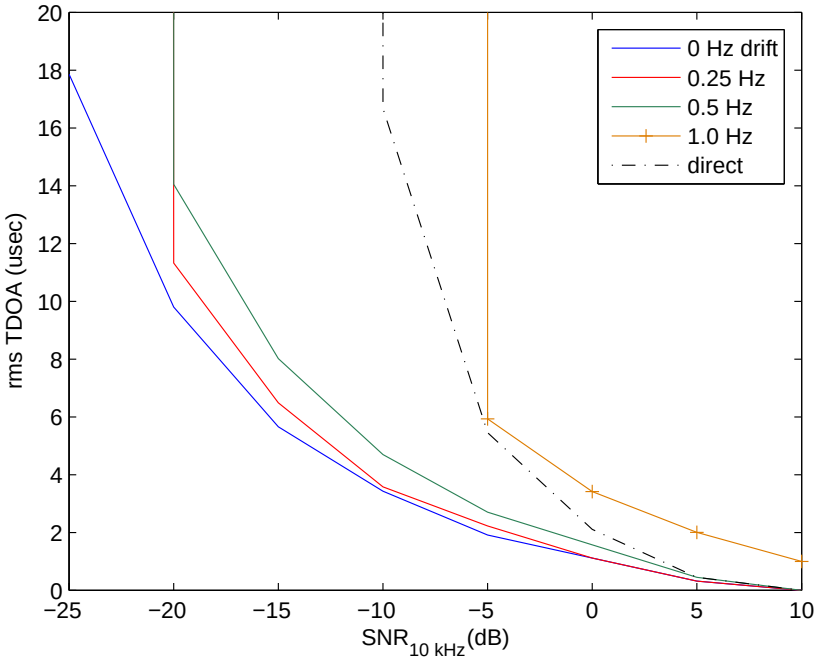


***Figure 7:*** *rms synthetic TDOA accuracy associated with an OOK signal with linear frequency drift.*

## 4.3 Mitigation of ambiguity due to frequency drift

Some mitigation of the ambiguity associated with carrier frequency drift is possible by simply excluding any TDOA estimates outside an assumed window of interest. For instance, the 0.5 sec ambiguity associated with the 1.0 Hz uncertainty in Figure 8 would likely be sufficiently different from expectation that would suggest it be discarded.

Additional mitigation is possible through employing some simple signal processing; an appropriate high pass filtering of the correlation function magnitude. Figure 9 compares the unfiltered correlation function magnitude for the 1.0 Hz drift example with that following high pass filtering with a single pole, Butterworth, high pass filter with corner frequency equal to $f_s/20000$. It is clear that the gross ambiguity associated with the carrier uncertainty has been removed. Figure 10 shows the improvement to the rms TDOA accuracy through the application of this high pass filtering. It can be seen that for low

[10]The 'true' peak is that which correctly reflects the true TDOA.

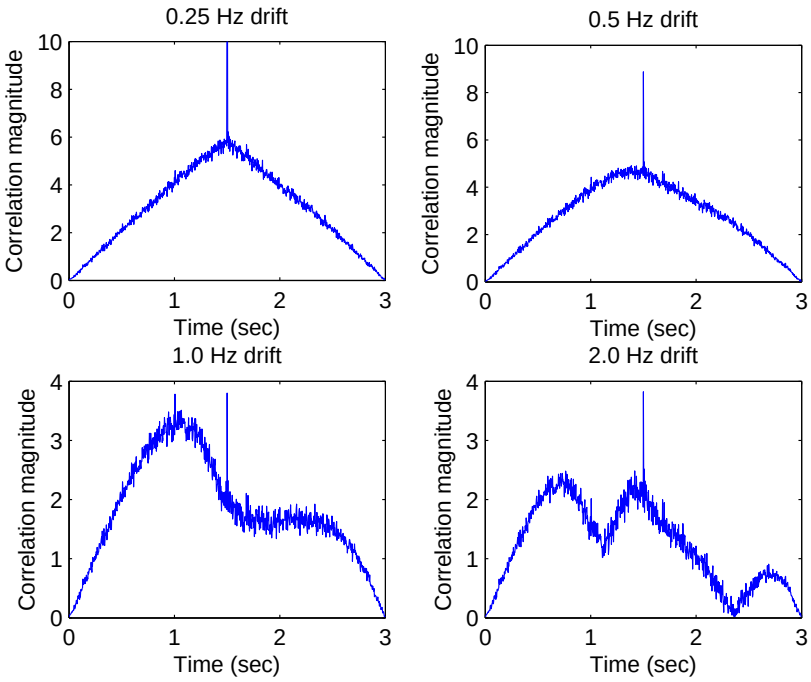


***Figure 8:*** *Magnitude correlation functions for linear carrier frequency drift.*

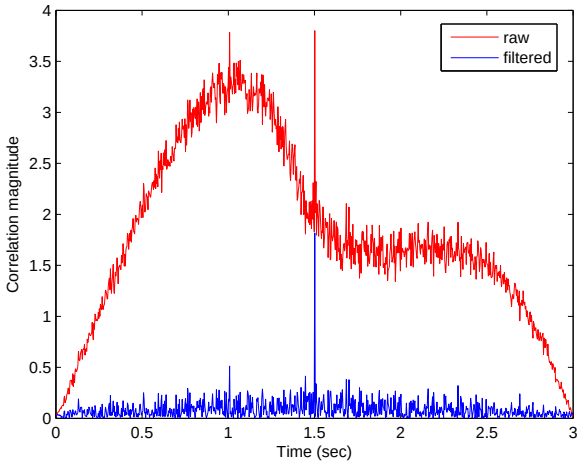


***Figure 9:*** *Magnitude correlation functions for 1.0 Hz linear carrier frequency drift with and without high pass filtering.*

SNR, the performance in the presence of 1.0 Hz carrier frequency drift (and even 2.0 Hz) is now better than the direct TDOA computation[11].

[11]That the knee in the Figure 10 curve depicting the TDOA accuracy for 0 Hz carrier drift occurs at -20 dB, yet there was no such knee depicted in Figure 7, reflects the subtle influence of the high pass filtering on the correlation function.

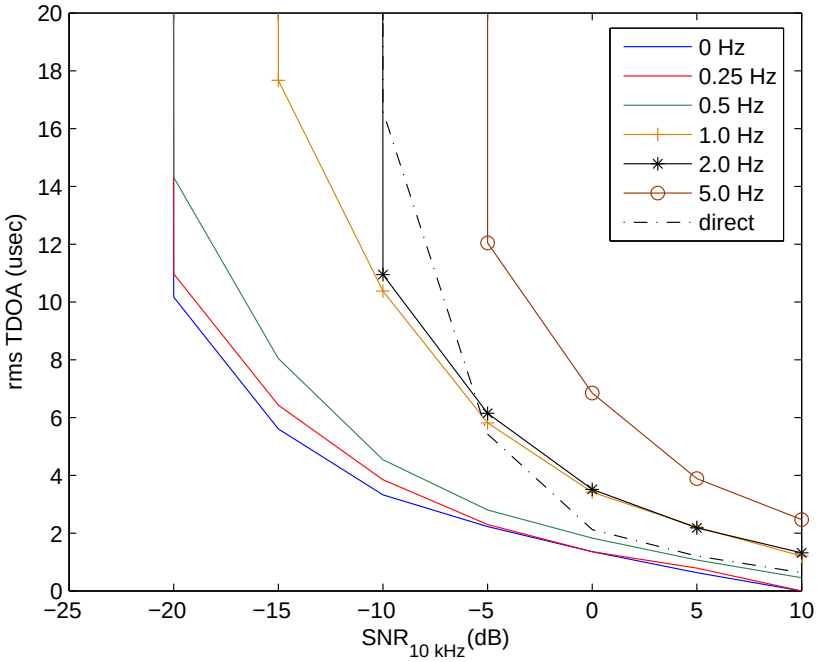


***Figure 10:*** *rms synthetic TDOA accuracy associated with an OOK signal with linear frequency drift, using high pass filtering of the correlation magnitude.*

## 4.4 Experimental trial results

Experimental trials were conducted using a radio frequency transmitter of interest, with parameters that match the simulated OOK source in section 3. Data was acquired at an SNR computed to be approximately equal to +10 dB within a 10 kHz bandwidth and white Gaussian noise was added to degrade the signal to the levels illustrated. A small amount of narrowband interference was also present on the original signal. The carrier was estimated from the argument of overlapping FFTs[12] and the frequency search range was restricted to 50 Hz about the approximately 0 Hz carrier. The experimental results in Figure 11 show a degree of performance difference between direct and synthetic estimation that is commensurate with the analysis and simulation results.

[12]FFTs using 1 second of data, overlapped by 87.5% and 4 times oversampled through zero padding.

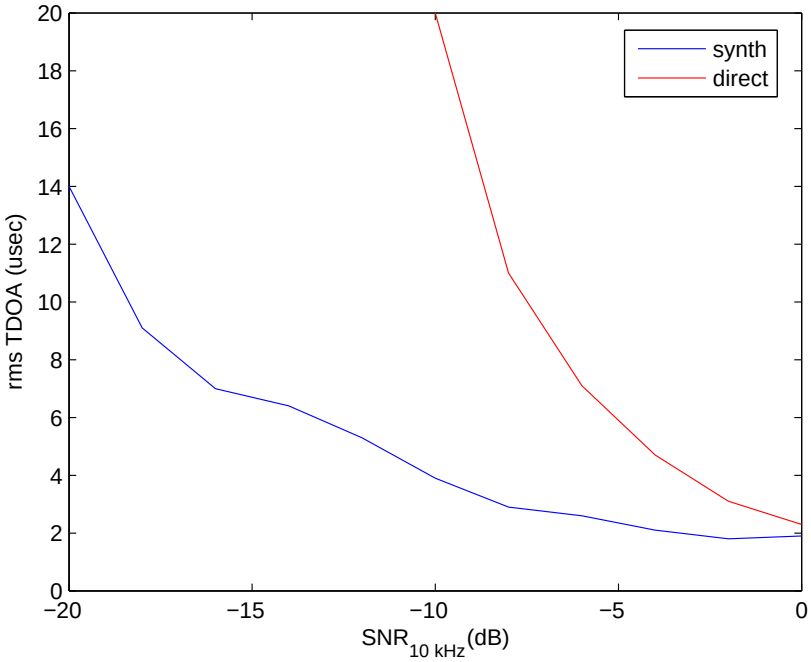


***Figure 11:*** *rms TDOA accuracy associated with an OOK signal received in a realistic RF environment.*

# 5 Conclusion

This report has developed analytical expressions for the variance bounds associated with the use of a prototype signal in a 'synthetic' estimation of time difference of arrival, with a focus on On-Off-Keyed signalling. Simulations have been conducted, which illustrate close agreement with theory and which suggest that under low SNR conditions, the accuracy with which TDOA can be estimated can be improved by an amount equivalent to in excess of a 10 dB SNR improvement. Some experimental results, using an RF transmission through a representative environment have been included, and show a similar degree of improvement.

# Acknowledgements

The authors would like to acknowledge Adrian Caldow, who strongly contributed through both general discussion and the development of the test transmitters. Don Simkins' input through discussions of performance expectations and experimental conduct was invaluable and is also acknowledged.

# References

1. A. B. Carlson. *Communication Systems*. McGraw-Hill, 1986.

2. C. H. Knapp and G. C. Carter. The generalized correlation method for estimation of time delay. *IEEE Transactions on Acoustics Speech and Signal Processing*, 24(4):320–327, August 1976.

3. S. Stein. Algorithms for ambiguity function processing. *IEEE Transactions on Acoustics Speech and Signal Processing*, 29(3):588–599, June 1981.

4. E. Weinstein and A. J. Weiss. Fundamental limitations in passive time-delay estimation - part ii: Wideband systems. *IEEE Transactions on Acoustics, Speech and Signal Processing*, ASSP-32(5):1064–1078, October 1984.

5. A. J. Weiss and Z. Stein. Optimal below threshold delay estimation for radio signals. *IEEE Transactions on Aerospace and Electronic Systems*, AES-23(6):726–730, November 1987.

# Appendix A Simplification of the Cramer Rao bound for TDOA estimation using complex envelopes

For the case where the signal and noise are restricted to within an IF bandwidth $\omega_0 \pm W/2$, where $\alpha = 1$ and for sufficiently high SNR [5] the Cramer Rao bound for the variance of the estimation of time delay using complex envelopes is given by [5]

$$\sigma^2_{min} = \left[ \frac{T}{2\pi} \int_{\omega_0 - W/2}^{\omega_0 + W/2} 2SNR(\omega)(\omega - \omega_0)^2 d\omega \right]^{-1}, \tag{A1}$$

where

$$SNR(\omega) = \frac{G_{ss}(\omega)/G_{n1n1}(\omega).G_{ss}(\omega)/G_{n2n2}(\omega)}{1 + G_{ss}(\omega)/G_{n1n1}(\omega) + G_{ss}(\omega)/G_{n2n2}(\omega)} \tag{A2}$$

and $G_{ss}(\omega)$, $G_{n1n1}(\omega)$ and $G_{n2n2}(\omega)$ are the signal and noise auto-spectra. This can be alternatively phrased in terms of frequency units of Hertz through a change of variables, $\omega = 2\pi f$ and using bandwidth $B$ Hz instead of $W$ rad/sec. Then the minimum variance is

$$\begin{aligned} \sigma^2_{min} &= \left[ \frac{T}{2\pi} \int_{fc - B_s/2}^{f_c + B_s/2} (2\pi)^2 2(f - f_c)^2 \frac{G_{ss}(f)/G_{n1n1}(f).G_{ss}(f)/G_{n2n2}(f)}{1 + G_{ss}(f)/G_{n1n1}(f) + G_{ss}(f)/G_{n2n2}(f)} d(2\pi f) \right]^{-1} \\ &= \left[ 4\pi^2 T \int_{fc - B_s/2}^{f_c + B_s/2} 2(f - f_c)^2 \frac{G_{ss}(f)/G_{n1n1}(f).G_{ss}(f)/G_{n2n2}(f)}{1 + G_{ss}(f)/G_{n1n1}(f) + G_{ss}(f)/G_{n2n2}(f)} df \right]^{-1}, \end{aligned} \tag{A3}$$

which is equivalent to

$$\sigma^2_{min} = \left[ 4\pi^2 T \int_{-B_s/2}^{B_s/2} 2f^2 \frac{\tilde{G}_{ss}(f)/\tilde{G}_{n1n1}(f).\tilde{G}_{ss}(f)/\tilde{G}_{n2n2}(f)}{1 + \tilde{G}_{ss}(f)/\tilde{G}_{n1n1}(f) + \tilde{G}_{ss}(f)/\tilde{G}_{n2n2}(f)} df \right]^{-1}, \tag{A4}$$

where $\tilde{G}_{ss}(f) = G_{ss}(f + f_c)$ etc.

Equation (A4) simplifies further, in a way the provides greater insight into the problem, as well as allowing a better comparison with commonly accepted literature [3] by considering the case where the noise spectra $\tilde{G}_{n1n1}(f) = N_1$ and $\tilde{G}_{n2n2}(f) = N_2$ are white within the bandwidth $B_s$ Hz. If the signal has total signal power $p$, then the signal to noise ratio associated with $x_1(t)$ and $x_2(t)$ is respectively $\gamma_1 = p/BN_1$ and $\gamma_2 = p/BN_2$, where $B \approx B_s$ is the equivalent noise bandwidth. Then we can write $\tilde{G}_{n1n1}(f) = p/B\gamma_1$ and $\tilde{G}_{n2n2}(f) = p/B\gamma_2$ so that

$$\frac{\tilde{G}_{ss}(f)/\tilde{G}_{n1n1}(f).\tilde{G}_{ss}(f)/\tilde{G}_{n2n2}(f)}{1+\tilde{G}_{ss}(f)/\tilde{G}_{n1n1}(f)+\tilde{G}_{ss}(f)/\tilde{G}_{n2n2}(f)} =$$

$$\begin{aligned}
&= \frac{\tilde{G}_{ss}^2(f)}{\tilde{G}_{n1n1}(f)\tilde{G}_{n2n2}(f)+\tilde{G}_{ss}(f)\tilde{G}_{n2n2}(f)+\tilde{G}_{ss}(f)\tilde{G}_{n1n1}(f)} \\
&= \frac{\tilde{G}_{ss}(f)}{\tilde{G}_{n1n1}(f)\tilde{G}_{n2n2}(f)/\tilde{G}_{ss}(f)+\tilde{G}_{n2n2}(f)+\tilde{G}_{n1n1}(f)} \\
&= \frac{\tilde{G}_{ss}(f)}{p^2/B^2\gamma_1\gamma_2\tilde{G}_{ss}(f)+p/B\gamma_1+p/B\gamma_2} \\
&= \frac{\tilde{G}_{ss}(f)}{(p/B)(p/(B\gamma_1\gamma_2\tilde{G}_{ss}(f))+1/\gamma_1+1/\gamma_2)} \\
&= \frac{B\tilde{G}_{ss}(f)}{p}\frac{\gamma_1\gamma_2}{p/B\tilde{G}_{ss}(f)+\gamma_1+\gamma_2}
\end{aligned} \tag{A5}$$

and

$$\begin{aligned}
\sigma_{min}^2 &= \left[4\pi^2 T\int_{-B_s/2}^{B_s/2} 2f^2\frac{B\tilde{G}_{ss}(f)}{p}\frac{\gamma_1\gamma_2}{p/B\tilde{G}_{ss}(f)+\gamma_1+\gamma_2}df\right]^{-1} \\
&= \left[4\pi^2 T\int_{-B_s/2}^{B_s/2} f^2\frac{B\tilde{G}_{ss}(f)}{p}\frac{2\gamma_1\gamma_2}{p/B\tilde{G}_{ss}(f)+\gamma_1+\gamma_2}df\right]^{-1} \\
&= \frac{p}{4\pi^2 TB}\left[\int_{-B_s/2}^{B_s/2} f^2\tilde{G}_{ss}(f)\gamma_{eq}(f)df\right]^{-1},
\end{aligned} \tag{A6}$$

where

$$\gamma_{eq}(f) = \frac{2\gamma_1\gamma_2}{p/B\tilde{G}_{ss}(f)+\gamma_1+\gamma_2} \tag{A7}$$

can be interpreted as an equivalent SNR associated with the generalised cross-correlation between $x_1(t)$ and $x_2(t)$.

# Appendix B Expressions for the mimimum variance of direct TDOA estimation

## B.1 White signal

If signal of interest and noise are both white over the bandwidth $-B/2$ to $B/2$ Hz then the minimum variance for the 'direct' estimation of TDOA can be obtained by observing that $\gamma_{eq}(f) = \gamma_{eq}$, $p = \int_{-\infty}^{\infty} G_{ss}(f)df$ and using the definition of 'rms radian frequency'

$$\beta = 2\pi \left[ \frac{\int_{-\infty}^{\infty} f^2 G_{ss}(f)df}{\int_{-\infty}^{\infty} G_{ss}(f)df} \right]^{1/2}. \tag{B1}$$

Then equation (A6) simplifies to

$$\sigma^2_{min} = \frac{1}{\beta^2 \gamma_{eq} TB}. \tag{B2}$$

and the equivalent SNR simplifies from (A7) to equation (7). Equation (B2) is the expression stated, without proof nor qualification of the conditions under which it applies, in [3].

## B.2 High SNR

If the SNR associated with the received signals is sufficiently high, then (A7) is approximately

$$\gamma_{eq} \approx \frac{2\gamma_1\gamma_2}{\gamma_1 + \gamma_2} \tag{B3}$$

which is again independent of frequency and again, the minimum variance for the direct TDOA estimation is given by (B2).

## B.3 Low SNR

If the SNR associated with the received signals is sufficiently low, then (A7) is approximately

$$\gamma_{eq}(f) \approx \frac{2\gamma_1\gamma_2 B G_{ss}(f)}{p}, \tag{B4}$$

which, unlike for the high SNR condition, is not independent of frequency. However, an expression for the minimum variance of the direct estimator, under this low SNR condition, that is independent of frequency can be derived by defining an alternative expression,

$$\tilde{\beta} = 2\pi \left[ \frac{\int_{-\infty}^{\infty} f^2 \tilde{G}^2_{ss}(f)df}{\left(\int_{-\infty}^{\infty} \tilde{G}_{ss}(f)df\right)^2} \right]^{1/2}. \tag{B5}$$

By substituting (B4) into (A6) and using (B5), it can be readily shown that for low SNR,

$$\sigma^2_{min} \approx \frac{1}{2\tilde{\beta}^2\gamma_1\gamma_2 TB^2}. \tag{B6}$$

The form here clearly differs from (B2) and illustrates an example of where the simple equations in [3] need to be treated with caution.

# Appendix C Bounds for the minimum variance of TDOA estimation from cross-correlation of a complex OOK signal

Two approaches are proposed here for the analysis of the bounds on the variance of TDOA estimation for a complex OOK signal. Both approaches recognise that an OOK signal can be considered as the sum of equal energy BPSK (binary phase shift keyed) and CW (continuous wave) signal components, but that the CW component makes no contribution to the TDOA estimation[13].

## C.1 Approach 1: Explicit consideration of BPSK signal component

In the first approach, the non-contribution of the CW component is explicitly included by computing the rms radian frequency $\beta$ based only on the BPSK component and correspondingly, making use only of the SNR associated with the BPSK component. Specifically, consider that the signal is bandlimited by the receiver to an RF bandwidth $B_s$ Hz, such that the complex envelope (complex baseband signal) has bandwidth approximately between $-B_s/2$ and $+B_s/2$ Hz. Then equation (B1) becomes

$$\beta_{BPSK} = 2\pi \left[ \frac{\int_{-\infty}^{\infty} f^2 G_{BPSK}(f) df}{\int_{-\infty}^{\infty} G_{BPSK}(f) df} \right]^{1/2} \tag{C1}$$

with $G_{BPSK}(f) = S_{BPSK}(f)|H(f)|^2$, where $S_{BPSK}(f) = \sin^2(\pi 2f/f_b)/(\pi 2f/f_b)^2$ [1], $f_b$ is the signalling rate and $H(f)$ is the filter frequency response. The SNR associated with the bandlimited BPSK signal $\gamma_{BPSK_{B_s}}$ can be deduced from $\gamma_{OOK_{B_s}}$, the SNR associated with the bandlimited OOK signal by considering that over infinite bandwidth, the power $\sigma^2_{OOK}$ in the OOK signal is $\sigma^2_{BPSK} + \sigma^2_{CW}$, where $\sigma^2_{BPSK} = \sigma^2_{CW}$. Define

$$\psi = \frac{\sigma^2_{BPSK_{B_s}}}{\sigma^2_{BPSK_\infty}} \tag{C2}$$

as the ratio of $\sigma^2_{BPSK_{B_s}} = \int_{-B_s/2}^{B_s/2} W_{BPSK}(f) df$, the power in the bandlimited BPSK signal to $\sigma^2_{BPSK_\infty} = \int_{-\infty}^{\infty} W_{BPSK}(f) df$, the wideband signal power. Then the power in the bandlimited OOK signal is

$$\begin{aligned} \sigma^2_{OOK_{B_s}} &= \sigma^2_{BPSK_{B_s}} + \sigma^2_{CW} \\ &= \psi \sigma^2_{BPSK_\infty} + \sigma^2_{BPSK_\infty} \\ &= (1+\psi)\sigma^2_{BPSK_\infty} \\ &= \frac{1+\psi}{\psi} \sigma^2_{BPSK_{B_s}} \\ \therefore \sigma^2_{BPSK_{B_s}} &= \frac{\psi}{1+\psi} \sigma^2_{OOK_{B_s}}. \end{aligned} \tag{C3}$$

[13]The correlation function between two tones of identical frequency has no distinct peak.

Since the same noise is common to both the whole OOK signal as well as the BPSK component, the SNR has the same relationship,

$$\gamma_{BPSK_{B_s}} = \frac{\psi}{1+\psi}\gamma_{OOK_{B_s}}. \tag{C4}$$

Equations (C4) and (C1) can then be used in conjunction with the appropriate expressions from sections 1 and 2 to realise the lower bound for the OOK signal.

## C.2 Approach 2: Exact expansion of the OOK expression

In this second approach, consider an explicit expansion of $\beta$ for the OOK signal,

$$\begin{aligned}
\beta_{OOK} &= 2\pi \left[ \frac{\int_{-\infty}^{\infty} f^2 G_{OOK}(f) df}{\int_{-\infty}^{\infty} G_{OOK}(f) df} \right]^{1/2} \\
&= 2\pi \left[ \frac{\int_{-\infty}^{\infty} f^2 (G_{BPSK}(f) + G_{CW}(f)) df}{\int_{-\infty}^{\infty} (G_{BPSK}(f) + G_{CW}(f)) df} \right]^{1/2} \\
&= 2\pi \left[ \frac{\int_{-\infty}^{\infty} f^2 G_{BPSK}(f) df + \int_{-\infty}^{\infty} f^2 G_{CW}(f) df}{\int_{-\infty}^{\infty} G_{BPSK}(f) df + \int_{-\infty}^{\infty} G_{CW}(f) df} \right]^{1/2}.
\end{aligned} \tag{C5}$$

Now, assuming that the CW signal component lies at exactly $f = 0$ Hz, the second numerator term vanishes. Also, it can be recognised that the denominator components are the power in each of the bandlimited BPSK and CW components. Equations (C2) and (C3) can be manipulated to show that these are related by $\sigma^2_{CW} = \sigma^2_{BPSK_\infty} = \sigma^2_{BPSK_{B_s}}/\psi$ so that (C5) simplifies to

$$\begin{aligned}
\beta_{OOK} &= 2\pi \left[ \frac{\int_{-\infty}^{\infty} f^2 G_{BPSK}(f) df}{(\psi+1)/\psi \int_{-\infty}^{\infty} G_{BPSK}(f) df} \right]^{1/2} \\
&= \sqrt{\frac{\psi}{\psi+1}} \beta_{BPSK}
\end{aligned} \tag{C6}$$

Equation (C6) can be used with the equivalent SNR for the (bandlimited) received OOK signal to bound the TDOA estimation accuracy.

The apparent inconsistency between this and 'approach 1' is reflected in Figure C1, which shows a significant disagreement for direct TDOA estimation using each of the two analytical approaches, applied to the OOK signal example from section 3.3. For computational simplicity, the Stein equations were used to generate curves for direct TDOA estimation using both approaches 1 and 2, respectively plotted using dash-dot and dashed line types. The red and black curves correspond to the respective use of a 'brick wall' and exact filter approximation in the computation of $\beta$, the noise bandwidth $B$ and, where applicable, $\gamma_{eq}(f)$. Simulation results are overlaid with the curves representing theory.

Most notable from Figure C1 is the considerable discrepancy between the two approaches to handling the OOK signal. This can be explained by considering that the

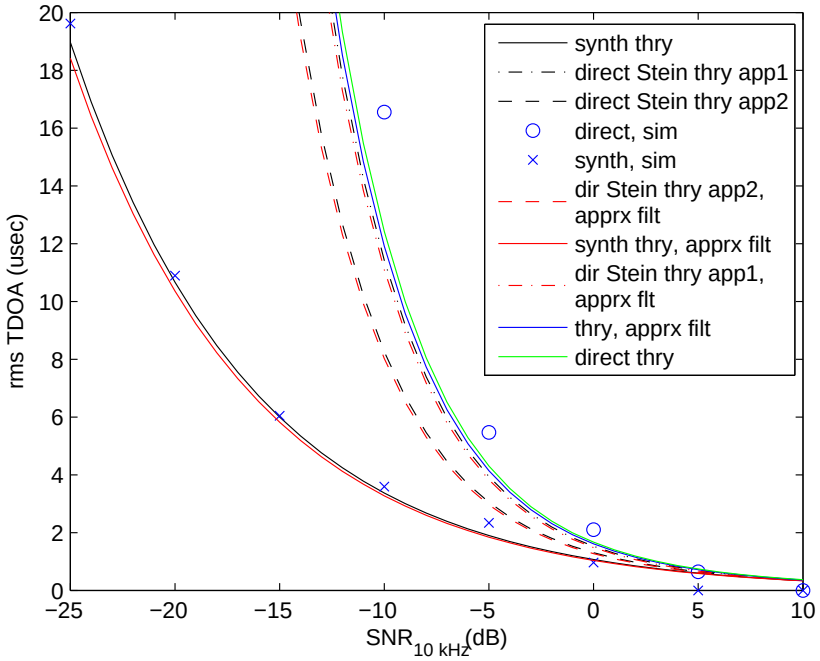


***Figure C1:*** *Theoretical and experimental rms TDOA accuracy associated with an OOK signal with 0 Hz carrier frequency. The red curves show the results when the receive filter is approximated by a 'brick wall' for the purposes of computation of $\beta$ and $B$.*

analytical lower variance bounds can only be achieved when the correlation is preceded by filtering that is proportional to the square root of the SNR spectral shape. In 'approach 1', the signal of interest is effectively a BPSK signal, which differs less from the rectangular filtering function used in the simulations than does an OOK spectral shape. Consequently, 'approach 1' yields a tighter lower variance bound for the direct correlation. With 'approach 1' established as the more accurate method, the curves for direct estimation using 'approach 1' and equations (5) and (6) are also included as solid lines, with blue and green colour respectively signifying the use of the approximate and exact filter responses respectively.

The curves shown in red and green have been included to explore the benefit of more accurately computing the rms radian frequency $\beta$ and confirm that, at least for the current parameters, there is little degradation to the accuracy of the analytical evaluations through using the more coarse filter approximation.

DISTRIBUTION LIST *

Reference Assisted TDOA Computation for On-Off Keyed Signals

Gareth Parker and John Homer

## AUSTRALIA

| **DEFENCE ORGANISATION** | **No. of Copies** |
|---|---|
| **S&T Program** | |
| Chief Defence Scientist<br>Chief, Projects and Requirements Division<br>DG Science Strategy and Policy | Doc. Data Sheet & Exec. Summary & Dist. List |
| Counsellor Defence Science, London | Doc. Data Sheet |
| Counsellor Defence Science, Washington | Doc. Data Sheet |
| Scientific Adviser to MRDC, Thailand | Doc. Data Sheet |
| Scientific Adviser Intelligence and Information | Doc. Data Sheet |
| Navy Scientific Adviser | Doc. Data Sheet & Dist. List |
| Army Scientific Adviser | Doc. Data Sheet & Dist. List |
| Air Force Scientific Adviser | Doc. Data Sheet & Dist. List |
| Scientific Adviser to the DMO | Doc. Data Sheet & Dist. List |
| Scientific Adviser - VCDF/CJOPS/Strategy | Doc. Data Sheet & Dist. List |
| Deputy Chief Defence Scientist (Information and Weapons Systems) | 1 |
| Chief of Command Control Communications and Intelligence Division | 1 |
| Research Leader Signals Intelligence | 1 |
| Task Leader, INT07/322 | 1 |
| Author: Gareth Parker | 1 Printed |
| Author: John Homer | 1 Printed |
| **DSTO Library and Archives** | |
| Library Fishermans Bend | Doc. Data Sheet |
| Library Edinburgh | 1 Printed |
| Library,Sydney | Doc. Data Sheet |
| Library, Stirling | Doc. Data Sheet |
| Library Canberra | Doc. Data Sheet |
| **Capability Development Group** | |
| Director General Maritime Development | Doc. Data Sheet |
| Director NCW Development | Doc. Data Sheet |
| Assistant Secretary Investment Analysis | Doc. Data Sheet |

| | |
|---|---|
| DICTF | Doc. Data Sheet |
| **Strategy Executive** | |
| Policy Officer, Counter–Terrorism and Domestic Security | Doc. Data Sheet |
| **Vice Chief of the Defence Force Group** | |
| SO (Science) Counter Improvised Explosive Device Task Force | Doc. Data Sheet & Exec. Summary & Dist. List |
| **Joint Logistics Command** | |
| Directorate of Ordnance Safety - Head Engineering Systems | Doc. Data Sheet |
| Director General Strategic Logistics | Doc. Data Sheet |
| **Navy** | |
| Maritime Operational Analysis Centre, Building 89/90 Garden Island Sydney NSW | Doc. Data Sheet & Dist. List |
| Deputy Director (Operations) | |
| Deputy Director (Analysis) | |
| Director General Navy Capability, Performance and Plans, Navy Headquarters | Doc. Data Sheet |
| Director General Navy Communications & Information Warfare | Doc. Data Sheet |
| Director General Navy Certification and Safety | Doc. Data Sheet |
| Head Navy Engineering | Doc. Data Sheet |
| Commodore Training | Doc. Data Sheet |
| Commander Surface Force | Doc. Data Sheet |
| Commander Mine Warfare, Clearance Diving, Hydrographic, Meteorological and Patrol Force | Doc. Data Sheet |
| Commander Fleet Air Arm | Doc. Data Sheet |
| Commander Submarine Force | Doc. Data Sheet |
| Commodore Flotillas | Doc. Data Sheet |
| Commodore Support | Doc. Data Sheet |
| SO Science Fleet Headquarters | Doc. Data Sheet |
| **Army** | |
| Australian National Coordination Officer ABCA (AS NCO ABCA), Land Warfare Development Centre, Puckapunyal | Doc. Data Sheet |
| SO(Science) Forces Command | Doc. Data Sheet |
| SO (Science) – Special Operations Command (SOCOMD) Russell Offices Canberra | Doc. Data Sheet & Exec. Summary & Dist. List |
| SO(Science) 1st Division | Doc. Data Sheet |
| SO2 S&T FDG LWDC – (Staff Officer for Science and Technology, Force Development Group) | Doc. Data Sheet |
| SO(Science) 1Bde | Doc. Data Sheet |
| SO(Science) 3Bde | Doc. Data Sheet |

| | |
|---|---|
| SO(Science) 17 CSS Bde | Doc. Data Sheet |
| J86 (TCS GROUP), DJFHQ | Doc. Data Sheet |
| **Air Force** | |
| SO (Science) – Headquarters Air Combat Group, RAAF Base, Williamtown NSW 2314 | Doc. Data Sheet & Exec. Summary |
| Staff Officer Science Surveillance and Response Group | Doc. Data Sheet & Exec. Summary |
| SO (Science) Combat Support Group | Doc. Data Sheet & Exec. Summary |
| Staff Officer Science HQ Air Lift Group | Doc. Data Sheet & Exec. Summary & Dist. List |
| **Intelligence and Security Group** | |
| AS Transnational and Scientific Intelligence, DIO | Doc. Data Sheet |
| Manager, Information Centre, Defence Intelligence Organisation | Doc. Data Sheet |
| Director Advanced Capabilities, DIGO | Doc. Data Sheet |
| **Defence Materiel Organisation** | |
| CoS GM Systems | Doc. Data Sheet |
| Program Manager Air Warfare Destroyer | Doc. Data Sheet |
| Guided Weapon & Explosive Ordnance Branch (GWEO) | Doc. Data Sheet |
| Director Engineering Operations; Land Engineering Agency (Michael Yates) | Doc. Data Sheet |
| CSIO | Doc. Data Sheet |
| Deputy Director Joint Fuel & Lubricants Agency | Doc. Data Sheet |
| Systems Engineering Manager<br>CBRNE Program Office, Land Systems Division | Doc. Data Sheet |
| **OTHER ORGANISATIONS** | |
| National Library of Australia | 1 |
| NASA (Canberra) | 1 |
| Library of New South Wales | 1 |
| **UNIVERSITIES AND COLLEGES** | |
| **Australian Defence Force Academy** | |
| Library | 1 |
| Head of Aerospace and Mechanical Engineering | 1 |
| Hargrave Library, Monash University | Doc. Data Sheet |

## OUTSIDE AUSTRALIA

**INTERNATIONAL DEFENCE INFORMATION CENTRES**

| | |
|---|---|
| US Defense Technical Information Center | 1 |

| | |
|---|---|
| UK Dstl Knowledge Services | 1 |
| Canada Defence Research Directorate R&D Knowledge & Information Management (DRDKIM) | 1 |
| NZ Defence Information Centre | 1 |

**ABSTRACTING AND INFORMATION ORGANISATIONS**

| | |
|---|---|
| Library, Chemical Abstracts Reference Service | 1 |
| Engineering Societies Library, US | 1 |
| Materials Information, Cambridge Scientific Abstracts, US | 1 |
| Documents Librarian, The Center for Research Libraries, US | 1 |
| International Technology and Science Center (ITSC) Library | 1 |
| SPARES | 4 Printed |

**Total number of copies: Printed: 7, PDF: 18.**

* In keeping with the DSTO Research Library's Policy on Electronic distribution of official series reports, unclassified, xxx–in confidence and restricted reports will be sent to recipients via DRN email as per the distribution list. Authors, task sponsors, libraries and archives will continue to receive hard copies.

| **DEFENCE SCIENCE AND TECHNOLOGY ORGANISATION DOCUMENT CONTROL DATA** | | | | 1. CAVEAT/PRIVACY MARKING |
|---|---|---|---|---|
| 2. TITLE<br>Reference Assisted TDOA Computation for On-Off Keyed Signals | | | 3. SECURITY CLASSIFICATION<br>Document (U)<br>Title (U)<br>Abstract (U) | |
| 4. AUTHORS<br>Gareth Parker and John Homer | | | 5. CORPORATE AUTHOR<br>Defence Science and Technology Organisation<br>PO Box 1500<br>Edinburgh, South Australia 5111, Australia | |
| 6a. DSTO NUMBER<br>DSTO–TR–2457 | 6b. AR NUMBER<br>AR–014–831 | 6c. TYPE OF REPORT<br>Technical Report | 7. DOCUMENT DATE<br>August 2010 | |
| 8. FILE NUMBER | 9. TASK NUMBER<br>INT02/322 | 10. SPONSOR | 11. No. OF PAGES<br>22 | 12. No. OF REFS<br>5 |
| 13. URL OF ELECTRONIC VERSION<br>http://www.dsto.defence.gov.au/corporate/reports/DSTO–TR–2457.pdf | | | 14. RELEASE AUTHORITY<br>Chief, Command, Control, Communications and Intelligence Division | |
| 15. SECONDARY RELEASE STATEMENT OF THIS DOCUMENT<br>*Approved for Public Release*<br>OVERSEAS ENQUIRIES OUTSIDE STATED LIMITATIONS SHOULD BE REFERRED THROUGH DOCUMENT EXCHANGE, PO BOX 1500, EDINBURGH, SOUTH AUSTRALIA 5111 | | | | |
| 16. DELIBERATE ANNOUNCEMENT<br>No Limitations | | | | |
| 17. CITATION IN OTHER DOCUMENTS<br>No Limitations | | | | |
| 18. DSTO RESEARCH LIBRARY THESAURUS | | | | |

19. ABSTRACT

This document considers the use of a partially known prototype signal to enhance the time difference of arrival (TDOA) computation for an On-Off Keyed (OOK) signal. It is shown through analysis and simulation that this approach can achieve a considerable reduction in the SNR threshold at which an acceptable rms TDOA spread can be achieved. For a signal transmitted with a carrier frequency that is stable within each observation interval, the threshold improvement can be in excess of 10 dB for a signal of practical interest. A similar degree of improvement was also observed for a signal with a carrier that exhibited frequency drift of up to 0.5 Hz within a 1.5 second interval. Analysis and simulation results are shown to be consistent with computations performed on data acquired from real transmitters.